U.S. DEPARTMENT OF COMMERCE
NATIONAL OCEANIC AND ATMOSPHERIC ADMINISTRATION
NATIONAL WEATHER SERVICE
NATIONAL METEOROLOGICAL CENTER

OFFICE NOTE 221

An Assessment of Analysis Performance

Ronald D. McPherson
Development Division

JULY 1980

I. Introduction

Previous lectures in this series have discussed the theory and application of the NMC global data assimilation system, as well as its antecedents and the data base it is asked to assimilate. The series concludes with this examination of the performance of the system in operational practice. A variety of statistical measures have been monitored routinely since the system was implemented in September 1978. Some of these are presented in the next section. For comparison, similar statistics from the previous system based on the Hough function spectral objective analysis are included.

A third section discusses the large-scale characteristics of the system in terms of zonally-averaged profiles of certain quantities such as zonal and meridional wind components, temperature, and moisture. These are compared to analogous quantities from climatology.

The fourth section illustrates specific examples of system performance as seen in a particular case. Vertical structure, relationship between mass and motion fields, and representation of extrema are examined along with a general discussion of the character, advantages, and disadvantages of the analyzed fields. Examples are given separately in the Northern and Southern Hemispheres and the Tropics.

A general review of the lecture series constitutes the final section.

II. Statistical Evaluation*

Beginning in February 1977, a program to routinely monitor the performance of NMC's Global Data Assimilation System was placed in operation. This program calculates the differences between the analyzed fields and radiosonde observations (analysis "fit") and between the short-range forecasts which are updated in the assimilation, and the same radiosonde data (forecast error). These calculations are done for several variables - geopotential height, temperature, wind, and relative humidity - and several standard isobaric levels. A number of networks of radiosonde stations are used, including the two used for illustration in this section. These are a Northern Hemisphere network of 102 stations (NH102) and a North American network of 110 stations (NA110). For any synoptic analysis time, the calculation consists of bilinearly interpolating values of a field - either forecast or analysis - from regular grid points to the locations of the radiosonde stations of the two networks. Differences are formed between the interpolated forecast or analyzed value and the observed value for all stations. These constitute the evaluation data base, upon which various statistical manipulations may be performed. Two are shown here: the mean algebraic difference (bias); and the root-mean-square (rms) difference. A selection of levels and parameters has been made in order to illustrate typical behavior without overwhelming the reader with an avalanche of numbers.

---

*Material presented in this section is adapted from Gerrity (1980).

Those shown are:

850 mb temperature
500 mb geopotential
250 mb wind speed

The mean and rms statistics for these levels and parameters cover the first eleven months of operation of the present data assimilation system, October 1978 through August 1979. For comparison, similar numbers are included for the period one year earlier - October 1977 through August 1978 - when the assimilation system was based the Hough function spectral objective analysis method.

Figure 1 presents the monthly mean bias in the 850 mb temperature for the analysis and forecast or "guess" for the NA110 network (a,b) and for the NH102 (c,d). In the analysis the temperature bias tends to be relatively small in the present system (marked "OI" in the diagram) during cold months, but too warm during the warm season. By contrast, the previous system (marked "Hough" in the diagram) shows little variability with time. It is possible that this difference arises because of the way temperature is calculated at these levels in the two systems. In the present system, temperature at a specific level is a diagnostic quantity derived by interpolation from the analysis of layer-mean temperatures. The analysis ignores the effect of water vapor on temperature, i.e., the difference between ambient and virtual temperature is neglected. In warm months, atmospheric moisture content is relatively higher, so that this effect - which would produce a warm bias - would be more pronounced. In contrast, the Hough system performs an explicit analysis of reported ambient temperature at 850 mb; this is insensitive to variations in moisture. It is worth noting in passing that both systems display consistently small ($<0.5°C$) positive biases at 500 mb and 250 mb. At 100 mb, a larger warm bias appears in the present system, which may be associated with improper correction of high level radiosonde temperature measurements for effects of solar radiation.

Comparison of the lower diagrams of Figure 1 with the upper ones reveals a characteristic behavior of the present NMC global prediction model: the tendency to reduce temperatures during the early portions of the forecast in the low levels. The effect is not large, but it is quite consistent and appears with both assimilation systems. It is thought that this behavior results from an imbalance in the model's physics. Typically, the integration begins with relatively little precipitation occurring due to a combination of weak initial vertical motion and underestimates of relative humidity in areas near saturation. Several hours of integration are required to adjust this initial imbalance. Meanwhile, the long-wave radiation calculations are steadily cooling the atmosphere. This is effect is inadequately compensated by the release of latent heat due to insufficient precipitation. Consequently, the net effect is a cooling of the model atmosphere during the first several hours. This suggests the importance of proper initial balance not only in the model dynamics but in its physical parameterizations as well.

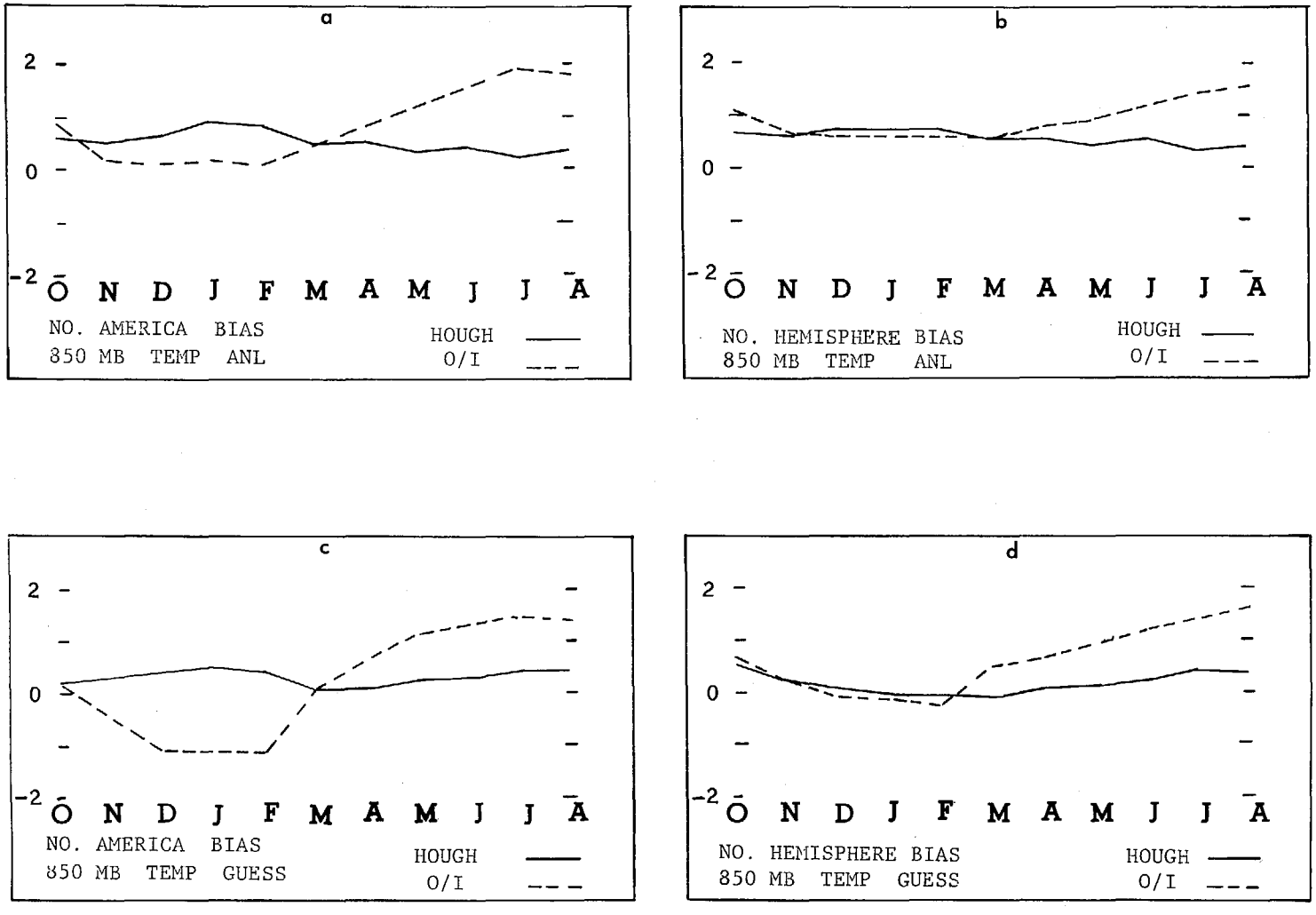

Figure 1. Monthly mean temperature bias error at 850 mb a. analysis, NA110 b. analysis, NH102 c. 6h forecast, NA110 d. 6h forecast, NH102

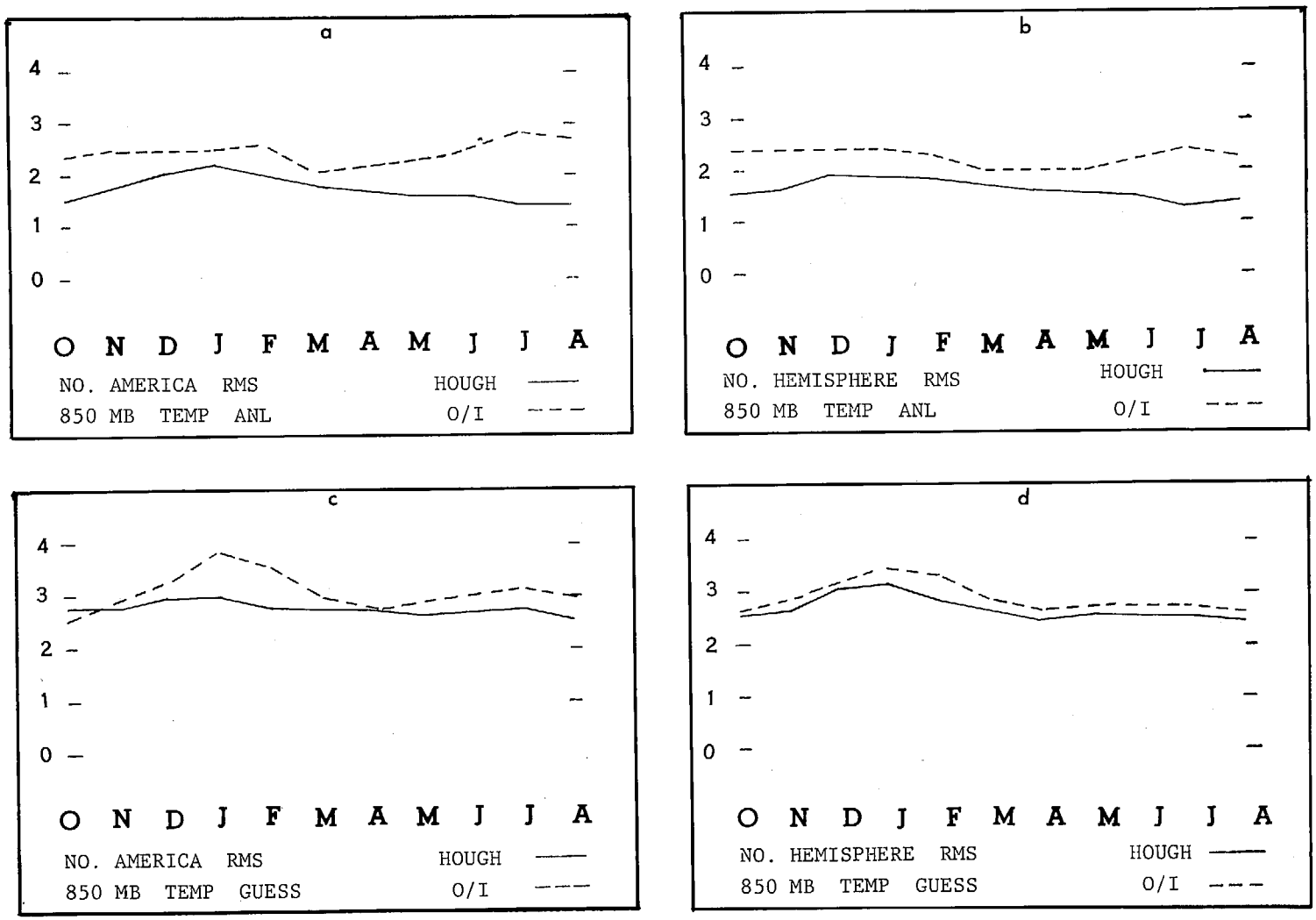

Figure 2. Monthly mean temperature rms error at 850 mb a. analysis, NA110 b. analysis, NH102 c. 6h forecast, NA110 d. 6h forecast, NH102

Figure 2 displays the rms temperature differences at 850 mb. These reflect the presence of the bias shown in Figure 3. It is worth noting that the difference between the two assimilation systems is smaller for the forecast than for the analysis.

Figure 3 presents the 500 mb geopotential height bias. In the analysis, the present system shows a very small (<5m) positive bias, possibly reflecting the warm temperature bias at lower levels, while the previous system exhibits a slight negative bias. Over the Northern Hemisphere as a whole, the guess has a cold bias, probably reflecting the forecast model's tendency to cool the model atmosphere. This effect is not so apparent in the NA110 network.

500 mb geopotential rms differences are presented in Figure 4. Over the NH102 network, there is essentially no difference in the degree to which the present analysis and the previous one fit the radiosonde data. This is somewhat surprising, since the Hough system directly analyzes 500 mb height at 500 mb, whereas the present system indirectly obtains 500 mb height fields by interpolation from the surface pressure, tropopause pressure, and layer-mean temperature analyses. It seems reasonable for the latter to not fit 500 mb height data as closely as the former, and this is indeed reflected in the NA110 network.

With respect to the verifications of the 500 mb height guess, a considerable difference is noted in the winter months over North America. The present system shows substantially higher errors in the 6h forecasts of 500 mb height. It is not clear whether this is due to a real difference between the systems, or to some other cause such as interannular variability. It is customary to observe a seasonal variation in these statistics, larger errors occurring in winter months. In this sense, the forecast scores from the Hough system over the NA110 network are anomalous: the January score is the lowest of the 11 month period. Other factors may also enter, such as the fact that during January and February of 1979 the assimilation cycle was frequently terminated prematurely because of computer problems. The existing recovery procedures were inadequate, leading to poor first guesses being used to restart the assimilation cycle. These problems were gradually solved, and it is possible that the improvement in forecast errors during the last several months reflects this.

Figure 5 presents the 250 mb rms wind speed errors: the bias statistic is not sufficiently interesting to include here. Both systems show a small negative bias at most levels; its magnitude is no more than 2 $msec^{-1}$ of 250 mb. Over the entire Northern Hemisphere, the present system exhibits smaller rms differences with observed radiosonde winds during the winter months than does the Hough system, both in the analysis and in the guess. The difference in the latter is especially pronounced. In the warm months, the reverse seems to be the case. These same features are also evident in the NA110 network, but to a lesser degree.

In summary, the statistical evaluation indicates that the present global data assimilation system appears to behave reasonably well, at least by comparison to its predecessor. It is worth noting that original intent

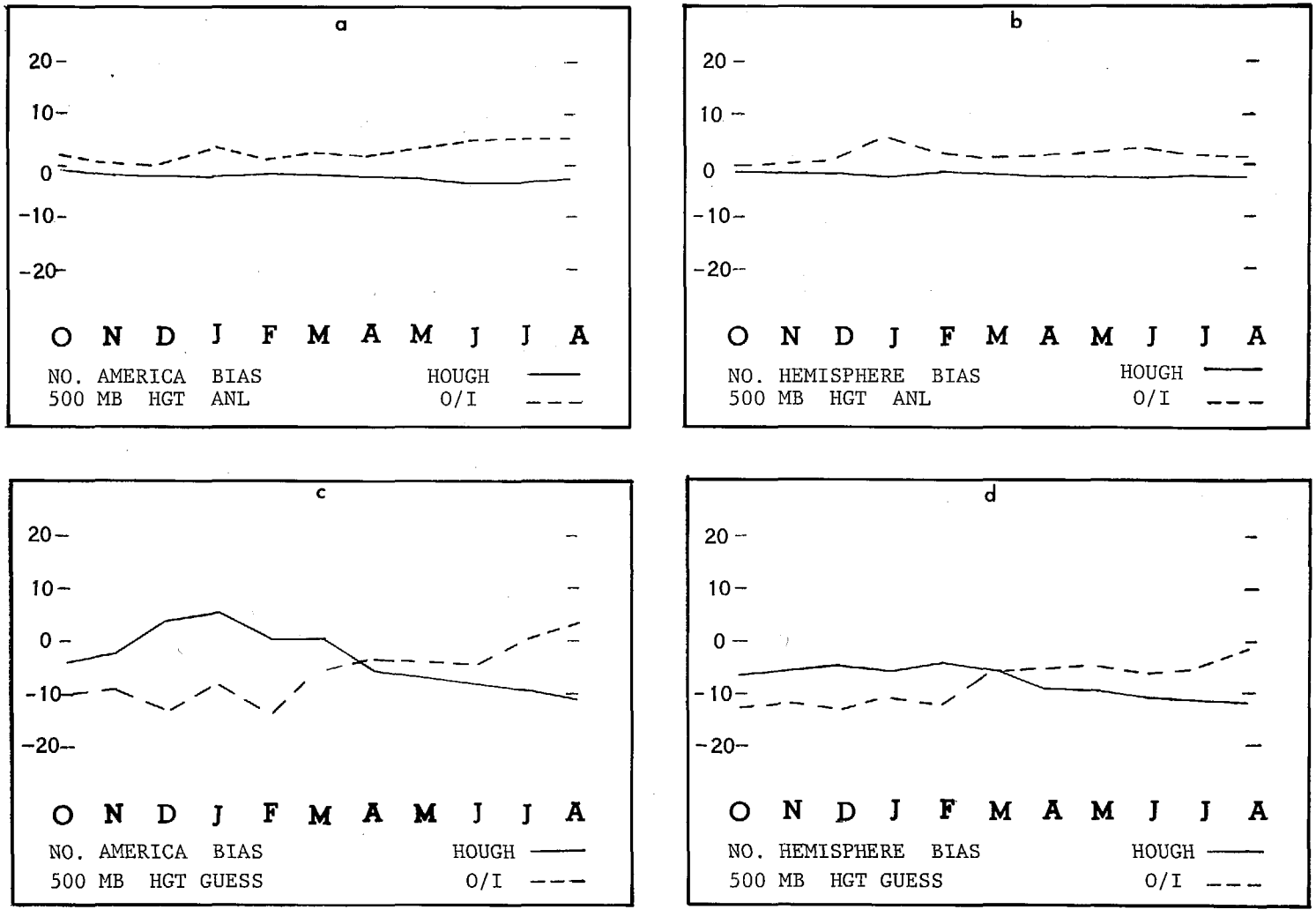

Figure 3. Monthly mean geopotential bias error at 500 mb a. analysis, NA110 b. analysis, NH102 c. 6h forecast, NA110 d. 6h forecast, NH102

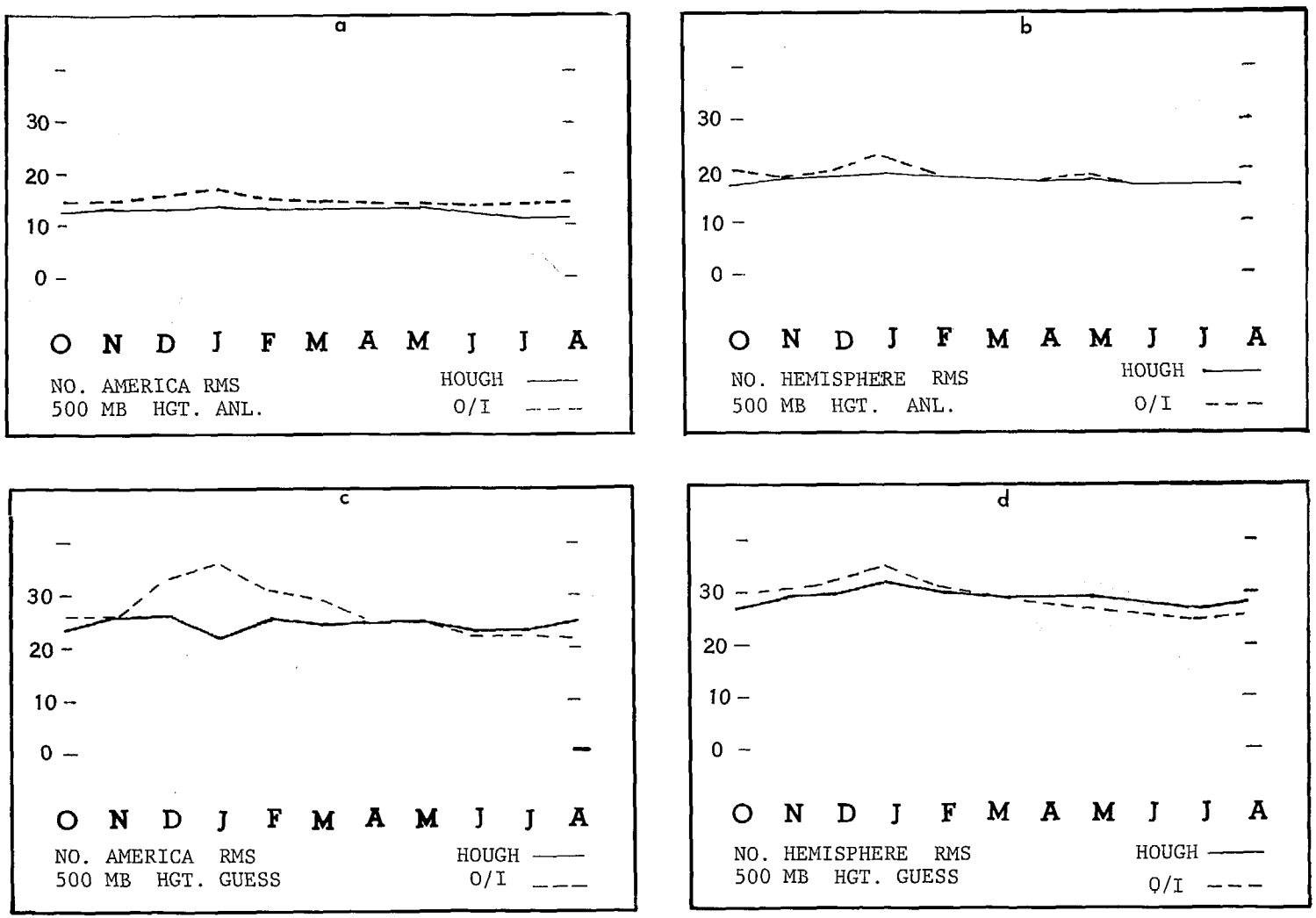

Figure 4. Monthly mean geopotential rms error at 500 mb a. analysis, NA110 b. analysis, NH102 c. 6h forecast, NA110 d. 6h forecast, NH102

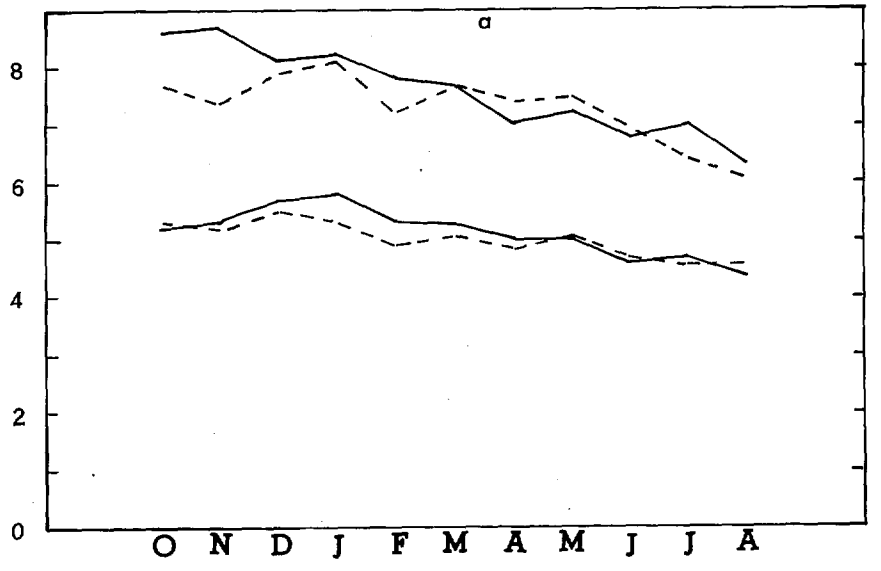

NO. AMERICA 110
250 MB RMS WIND SPEED
ANL & FIRST GUESS

HOUGH ——
O/I - - -

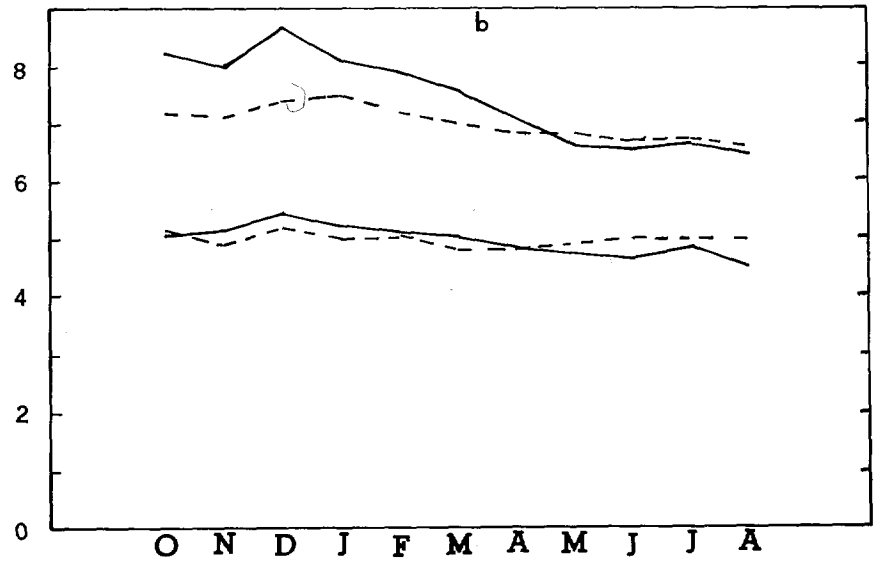

NO. HEMISPHERE 102
250 MB RMS WIND SPEED
ANL & FIRST GUESS

HOUGH ——
O/I - - -

Figure 5. Monthly mean rms wind speed error at 250 mb a. NA110 b. NH102

of the present system was to improve performance with respect to the remotely-sensed data over oceanic areas, while at least not degrading performance over data-rich continental areas. The preceding statistical evaluation suggests that the latter has been attained; an evaluation with respect to the former awaits new impact tests of the type described in the previous lecture.

III. Large-Scale Performance*

Statistical evaluation provides insight into the gross behavior characteristics of the assimilation system. We now refine the investigation by enquiring as to whether the large-scale characteristics of the system, as represented by zonally-averaged quantities, are reasonably well-behaved. The analyzed fields of temperature, wind, and relative humidity for 0000 GMT 6 January 1979 have been averaged around latitude circles and the results displayed on latitude vs. pressure diagrams. Figure 6 presents the zonally-averaged temperature field. In its major aspects, it agrees quite well with the January climatology, as may be found in Lorentz (1967). For example, the low-level maximum of near 300°K in the tropics, the very cold tropical statosphere, the reversal of the meridional temperature gradient with altitude, all may be found in a climatological representation. Some of the minor perturbations at high latitudes represent transient disturbances which would not appear in a temporal average. It is comforting to note that the main baroclinic zone is more intense in the winter hemisphere.

The zonal wind profile for this case is displayed in Figure 7. Westerly jet streams are featured at about the correct latitudes and pressures according to climatology although the winter hemisphere jet core is slightly equatorward and that of the summer hemisphere at a slightly lower altitude than the climatology would suggest. The winter hemisphere jet is more intense. Relatively strong tropical easterlies are apparent, extending to above 500 mb, and lighter easterlies are present in very high latitudes. These features are also in general agreement with climatology. However, tropical stratospheric easterlies which appear in climatology are not present in Figure 7.

Figure 8 presents a representation of the zonally-averaged meridional wind component. To construct this diagram, the actual meridional wind components were first represented spectrally by spherical harmonics. Truncated wind fields were then reconstructed using only nine functions. The resulting winds representing the large and medium scales were then averaged around latitude circles. In the diagram, the values have been multiplied by 10, so that a value of 15 represents 1.5 m/s. Several features are noteworthy. There is a suggestion of a Hadley circulation, especially in the winter hemisphere. Note the shallow low level equatorward flow from about 25N to the equator, with a deep layer of poleward flow above about 700 mb. Weaker evidence of a Hadley cell exists in the summer hemisphere.

---

*Material in this section adapted from unpublished notes by J.P. Gerrity (1979).

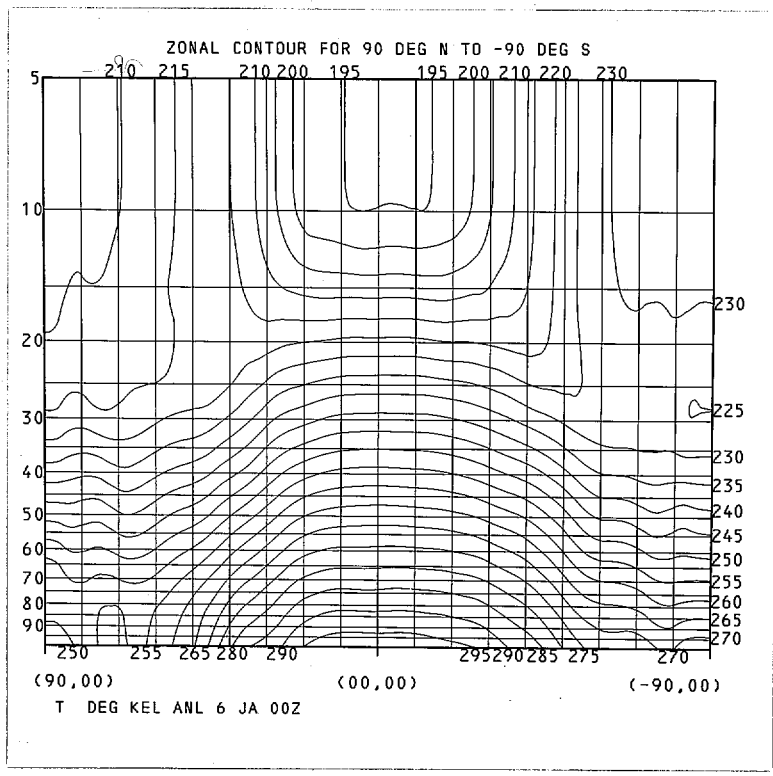

Figure 6. Temperature (degrees K) as a function of pressure, averaged around latitude circles. The ordinate is pressure in centibars, the absicissa latitude. Contour interval is 5°K. Date is 0000 GMT 6 January 1979.

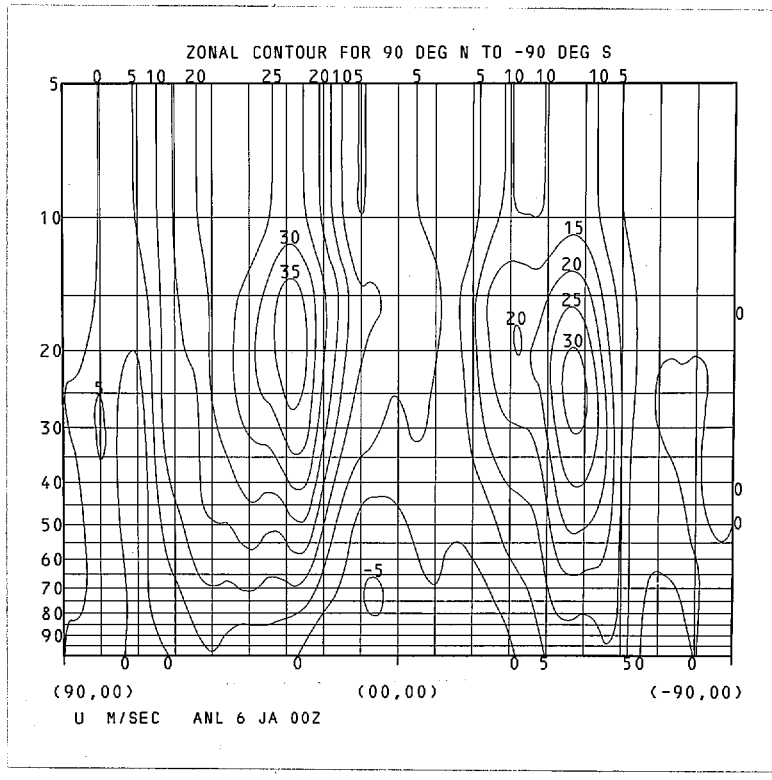

Figure 7. Zonal wind component (m/s) as a function of pressure, averaged around latitude circles. Contour interval is 5 m/s. Date is 0000 GMT 6 January 1979.

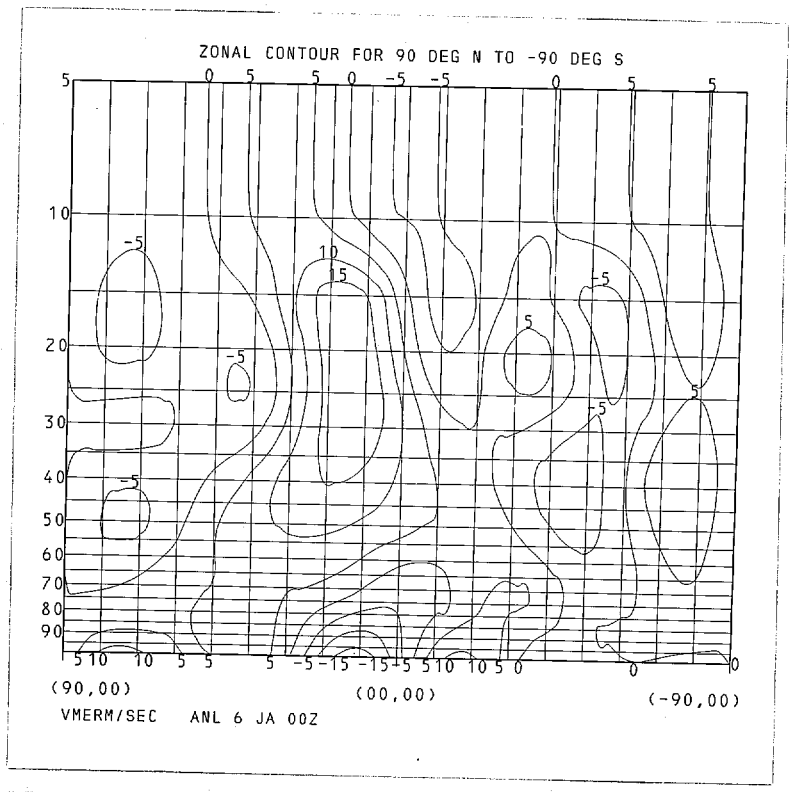

Figure 8. Meridional wind component (m/s) as a function of pressure, averaged around latitude circles, after representation by nine spherical harmonic functions. Values in m/s have been multiplied by 10, so that 15 represents 1.5 m/s. Date is 0000 GMT 6 January 1979.

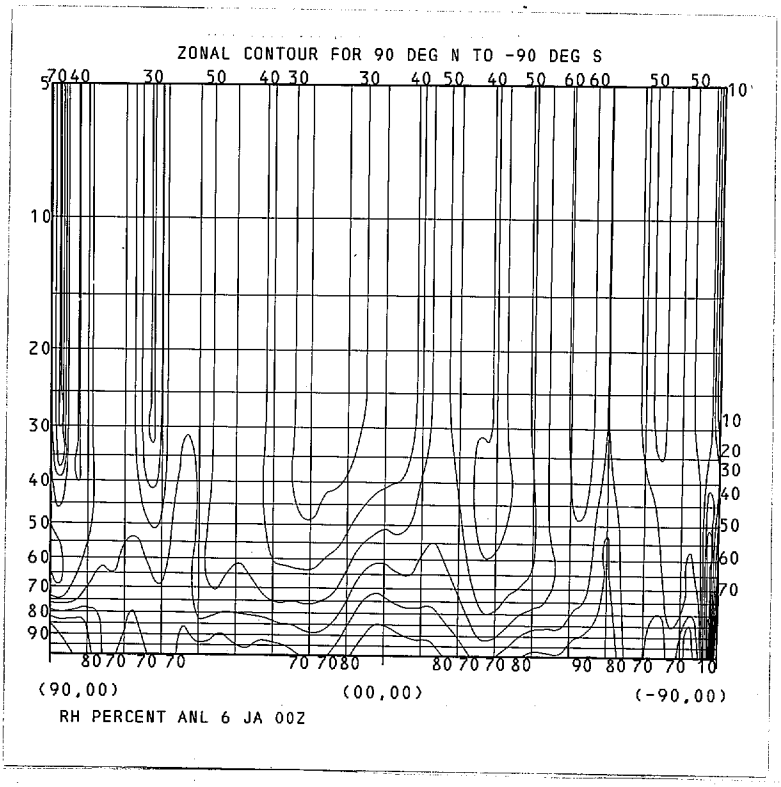

Figure 9 . Relative humidity (percent) as a function of pressure, averaged around latitude circles. Contour interval is 10%. Date is 0000 GMT 6 January 1979.

Zonally-averaged relative humidity for this case is depicted in Figure 9. The reader is cautioned to remember that moisture is a history variable only in the lowest 5 layers of the assimilation model, or only up to about 300 mb. Contours at higher levels in Figure 9 are therefore meaningless. In the tropics, the depth of the moist layer is somewhat greater than is suggested by climatology. There is an obvious difficulty near the South Pole, at least partially associated with reduction beneath the Antartic Plateau, which results in excessively moist representations. We note also deep moist towers near 55° latitude in both hemispheres, both of which are likely too intense. Thus, although the main features of the meridional moisture distribution are reasonable, the representation is too moist overall.

We conclude that the assimilation system produces analyses which depict meridional profiles of zonally-averaged quantities in general agreement with climatology.

IV. Examples of Performance Characteristics

Surface Pressure

One of the more unusual aspects of the NMC assimilation system is its treatment of surface pressure. It is therefore reasonable to enquire as to efficacy of this treatment. Figure 10 displays the Northern Hemisphere model terrain, in terms of the standard pressure at the elevation of the model grid point. The particular field shown derives from an original set of terrain heights (Smith, et al., 1968) at 1° latitude-longitude intervals, then represented spectrally and reconstructed on the grid using 24 spherical harmonic functions. This accounts for the broadening of the terrain field over the oceans adjacent to the continents. The spectral representation also accounts for the reflection of the narrow range of high mountains over Alaska as less high mountains over the Gulf of Alaska, and other similar aberrations.

When the standard pressure field of Figure 10 is subtracted from the actual model terrain pressure the resulting field of departure values appears as in Figure 11, for 1200 GMT 21 October 1979. For comparison, Figure 12 shows the corresponding field of pressure reduced to mean sea level. Over the oceans, of course, the only difference is the labeling of the contours. Over the continents, even near high terrain, the patterns depicted in Figures 11 and 12 differ only in detail. Perhaps the most prominent difference is the separate high pressure center over Greenland in the mean sea level pressure chart, which does not appear in the departure field. This is typical of problems associated with pressure reduction under extremely cold conditions. It may be concluded that this treatment of surface pressure not only is adequate for the purposes of the assimilation system, but may have some advantages for display as well.

Vertical Structure

Figure 13 displays the 1000 mb - 500 mb thickness pattern (dashed lines) superimposed on the mean sea level isobars, in order to gain an appreciation of the vertical structure of the atmosphere as represented

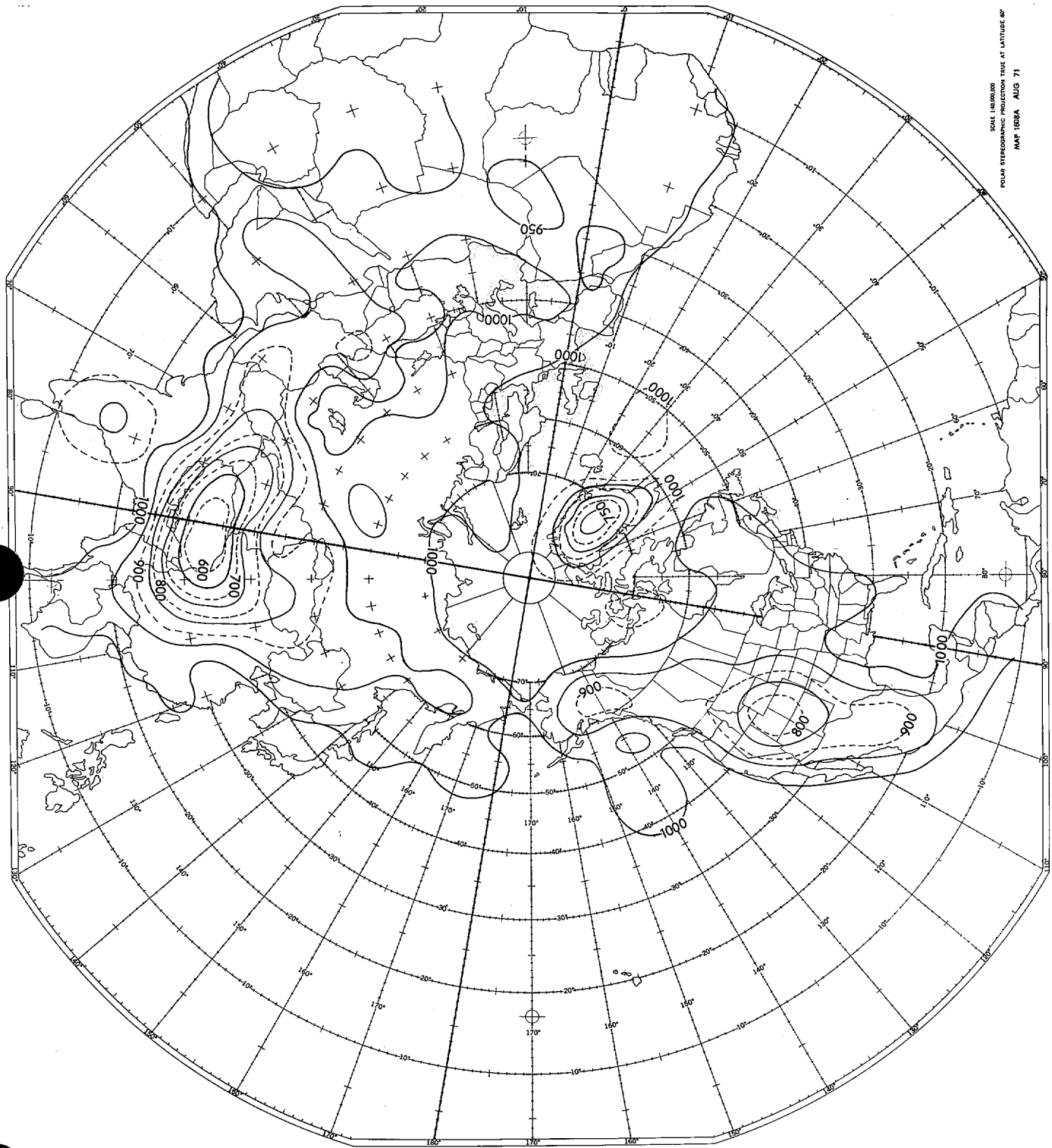

Figure 10. Standard atmosphere pressure at model terrain level in the NMC global data assimilation system. Contour interval is 50 mb.

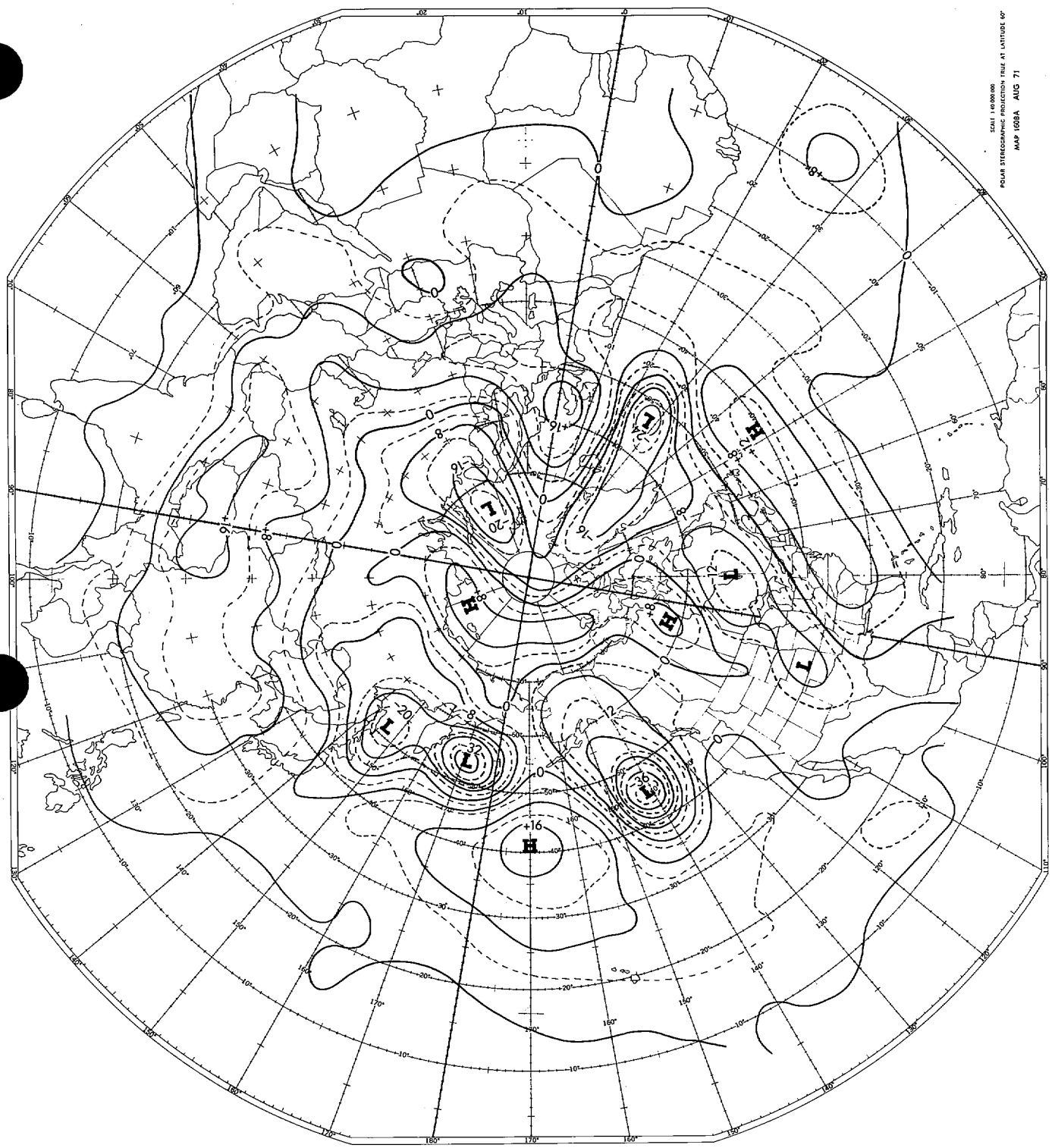

Figure 11. Analyzed deviations of model surface pressure from the standard atmosphere. Contour interval is 8 mb; intermediate contours are dashed. Date is 1200 GMT 21 October 1979.

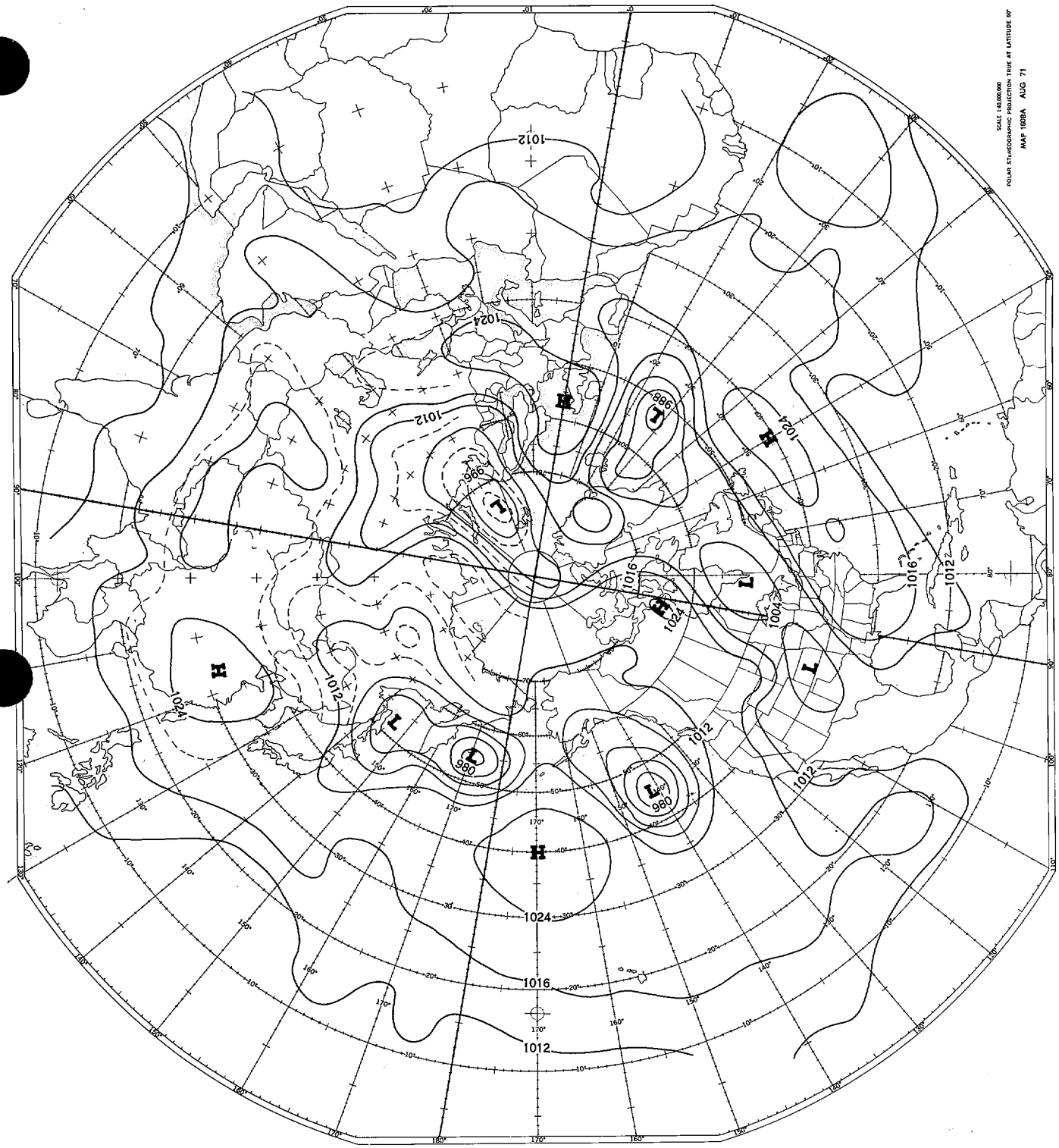

Figure 12. Model station pressure reduced to mean sea level for 1200 GMT 21 October 1979. Contour interval is 8 mb; some intermediate isobars are dashed. Unsmoothed.

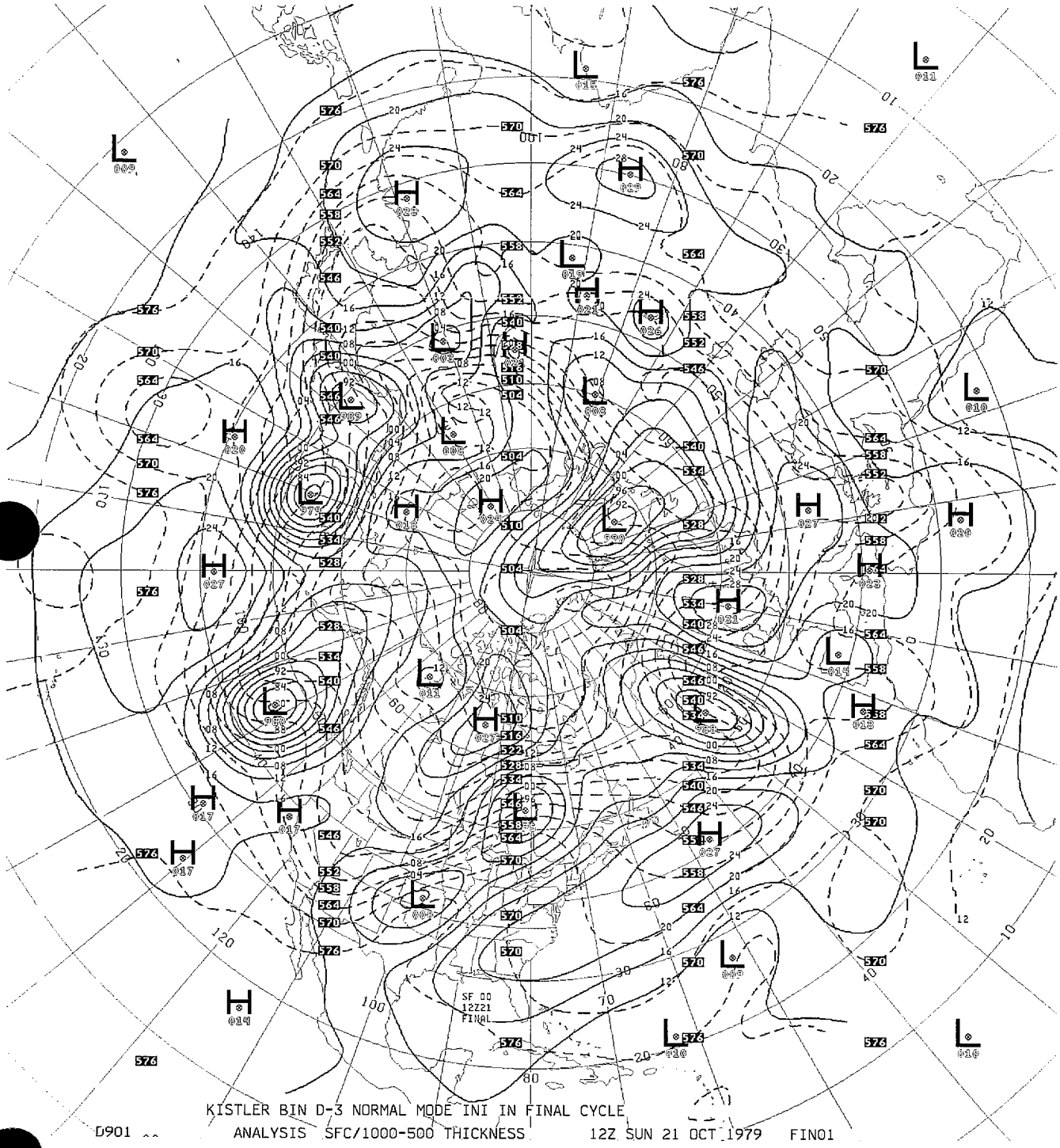

Figure 13. Mean sea level pressure (solid lines, contour interval 4 mb) and 1000-500 mb thickness (dashed lines, contour interval 60 m) for 1200 GMT 21 October 1979.

by the assimilation system. It is normally expected that cyclones at the earth's surface should be located a few degrees latitude to the west of the maximum anticyclonic curvature in the thickness pattern, so that warm air exists in advance of the system and cold air in its rear. The major cyclones near 30W and 140W and the developing storms over eastern North America and the Sea of Okhotsk exhibit this behavior. However, the major storm near 170E does not; it is nearly vertical through 500 mb as shown on Figure 14. The representation is well supported by the data, especially the northeast wind at the station just east of Kamchatka (Nicolaskoye; 55N, 166E).

Little support aloft is indicated in Figure 14 for the surface low pressure center near 51N, 120E. The flow pattern is rather strong northwesterly in this area. Upstream, an extremely short wave length trough-ridge system is depicted near 55N, 60E, well supported by the observations.

Figure 15 is an example of the quality and distribution of remote sounding data from satellites. Once again, this is from the case of 1200 GMT, 21 October 1979. The feature near 48N, 144W was undergoing extremely rapid cyclogenesis of this time. Note that the remote soundings define the system quite well.

Winds

Figure 16 shows the height contours and isotachs interpolated to the 250 mb level for 1200 GMT 21 October 1979. Superimposed are the observations available at or near the 250 mb level. This includes radiosondes (marked by circles), aircraft (boxes), and cloud-motion vectors (stars). For legibility, not all data have been plotted. Much of the remote sounding data is missing for this reason. One important point made by this diagram is the enormous quantity of data poleward of about 20N. With this kind of data base, a serious analysis error such as completely omitting a major system is a truly rare event.

At least two points are worth noting with respect to flow over east Asia: first, the depiction of the major jet stream core over Japan does not quite capture the maximum wind speeds. In spite of several observations near 130 kt, the analysis does not produce a 130 kt isotach, although values close to that could be inferred from the size of the 110 kt isotach. Underestimation of maximum wind speeds in strong jet streams is a typical analysis problem, resulting partly from inadequate resolution and partly from filters operating on the analysis to make the depictions smooth and attractive.

Second, it will be noted that the wind analysis, as depicted by the isotachs, responds to observed winds rather than the gradient of the mass field. This is especially noticeable in regions of strong curvature, such as 55N, 135E. The reported winds are near 30 kt in that area, and the analysis actually produces an area centered near 58N, 138E of less than 30 kt wind speed. Geostrophic wind speeds, would have been much higher. These points are confirmed in the vicinity of the cyclonic feature near 50N, 145W.

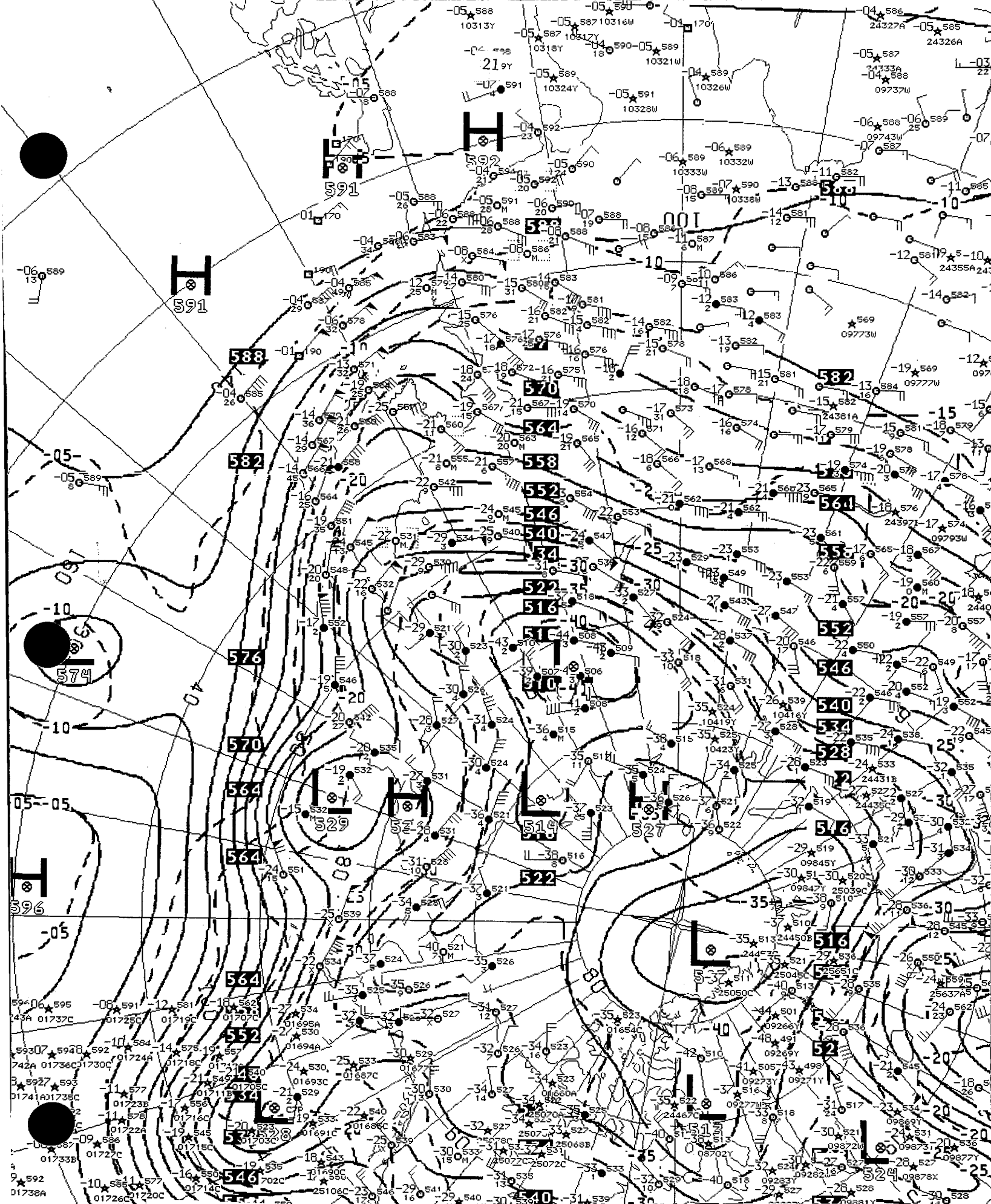

Figure 15. 500 mb geopotential (solid lines, 60 m interval) and temperature (dashed lines 5°K interval) for 1200 GMT 21 October 1979, over the north Pacific Ocean.

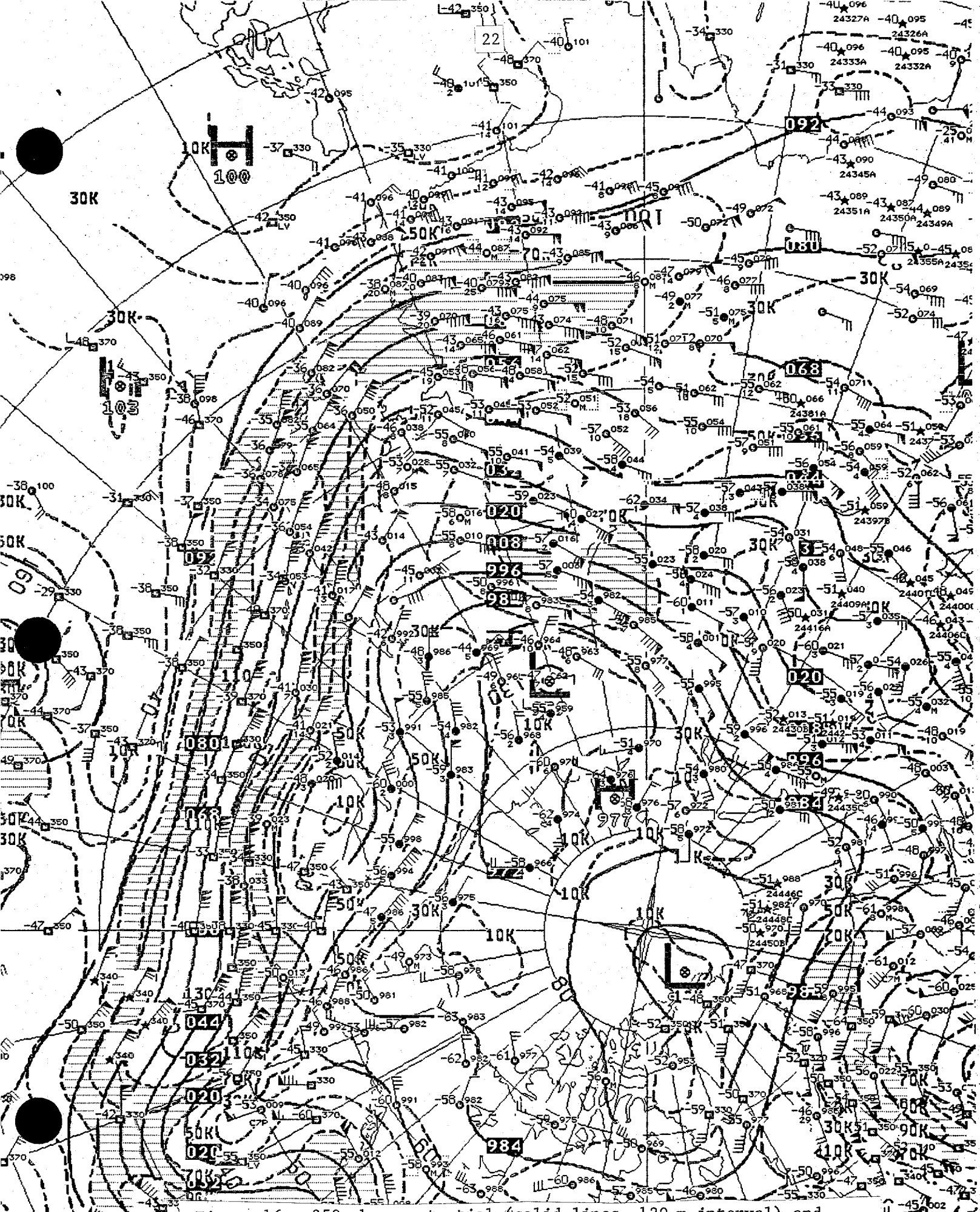

Figure 16, 250 mb geopotential (solid lines, 120 m interval) and isotachs (dashed lines, 20K interval) for 1200 GMT 21 October 1979 over the north Pacific Ocean.

Figures 17 and 18 show the vertical structure of the wind analysis. The diagrams are vertical cross-sections of the zonal wind component (dashed lines) and potential temperatures, for east Asia (110E) and the eastern Pacific (140W) respectively. In Figure 17, one can note the polar jet centered near 250 mb just poleward of 50N, and the stronger (greater than 40 m sec^{-1}) subtropical jet analyzed higher (200 mb) and just poleward of 30N. The zone of midtropospheric easterlies at high latitudes can also be seen. These features also appear on Figure 16. Figure 17 demonstrates that the analysis is vertically consistent. It is interesting to note in Figure 18 that although cyclogenesis is proceeding rapidly near 50N, 140W, the isentropes do not yet show appreciable distortion but a well-developed zone of low-level easterlies is apparent to the north of the center.

Southern Hemisphere

The NMC assimilation system is global in domain, and consequently examples of its performance in the Southern Hemisphere are necessary for completeness. Figure 19 shows the 1000 mb - 500 mb thickness pattern superimposed on the mean sea level pressure isobars, also for the case of 1200 GMT 21 October 1979. The patterns are smooth and coherent, and undoubtedly benefit from the remote sounding data and buoy reports. In terms of vertical structure, the developing cyclones near the Cape of Good Hope and west of Tasmania display the expected relationship between surface position and thermal pattern. However, there are other features which imply unusual vertical structure at least, or outright analysis errors at worst.

Tropics

A typical analysis in the tropics is shown in Figures 20 and 21, 850 mb and 250 mb streamlines and isotachs on a Mercator projection. The case is again 1200 GMT 21 October 1979. The 850 mb flow pattern is generally reasonable, showing a rather well-defined zone of easterlies between 5N and 20N throughout the longitudinal extent of the diagram. This flow is reasonably reflective of the available data, mostly radiowinds and cloud-motion vectors. Likewise, where data exist in the Southern Hemisphere tropics, the analysis is adequate. However, in those areas where no data exist, such as between 70E and 100E in the equatorial zone, the streamline field as depicted must be regarded as suspect.

At 250 mb, Figure 21 shows some interesting ciculation features. Note the weak cyclonic disturbance near Malaysia: it is well supported by the observed winds, yet is not reflected at all in the low levels, as may be seen in Figure 20. Further west, the analysis indicates an anticyclonic circulation just east of Sri Lanka. This is relatively well defined by the data. Between these two centers, the analysis suggests considerable cross-equatorial flow. This flow feeds into a moderately strong low-latitude jet stream in the Southern Hemisphere, eastward from about 120E. Finally, a large area of light winds--less than 10 kt-- may be noted from 10S to 20N, between roughly 150E and 160E. There are no data to confirm or deny this analysis.

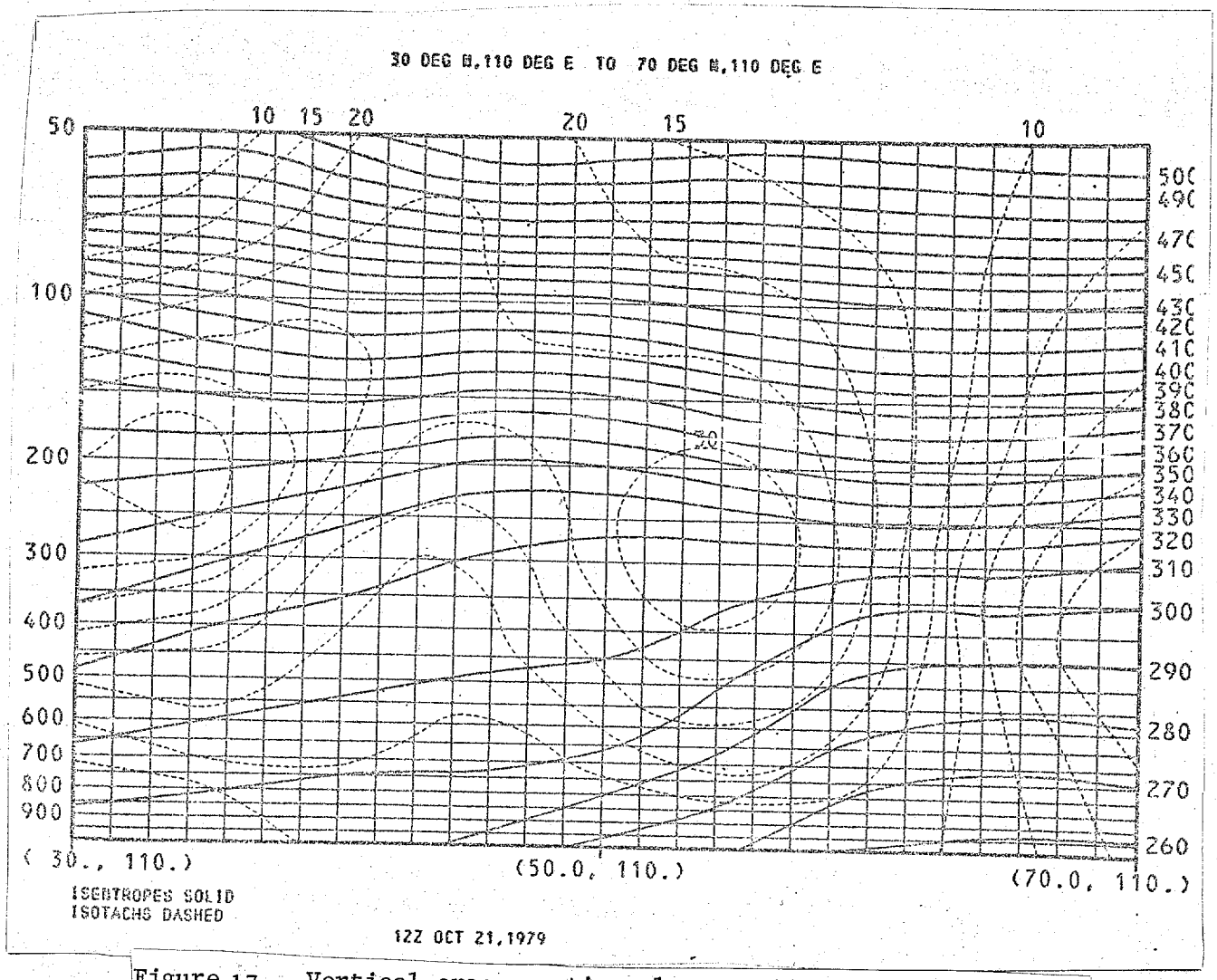

Figure 17. Vertical cross-section along meridian 110E between 30N and 70N. Solid lines are isentropes at 10°K intervals. Dashed lines represent zonal wind component at 5 m/s intervals. 1200 GMT 21 October 1979.

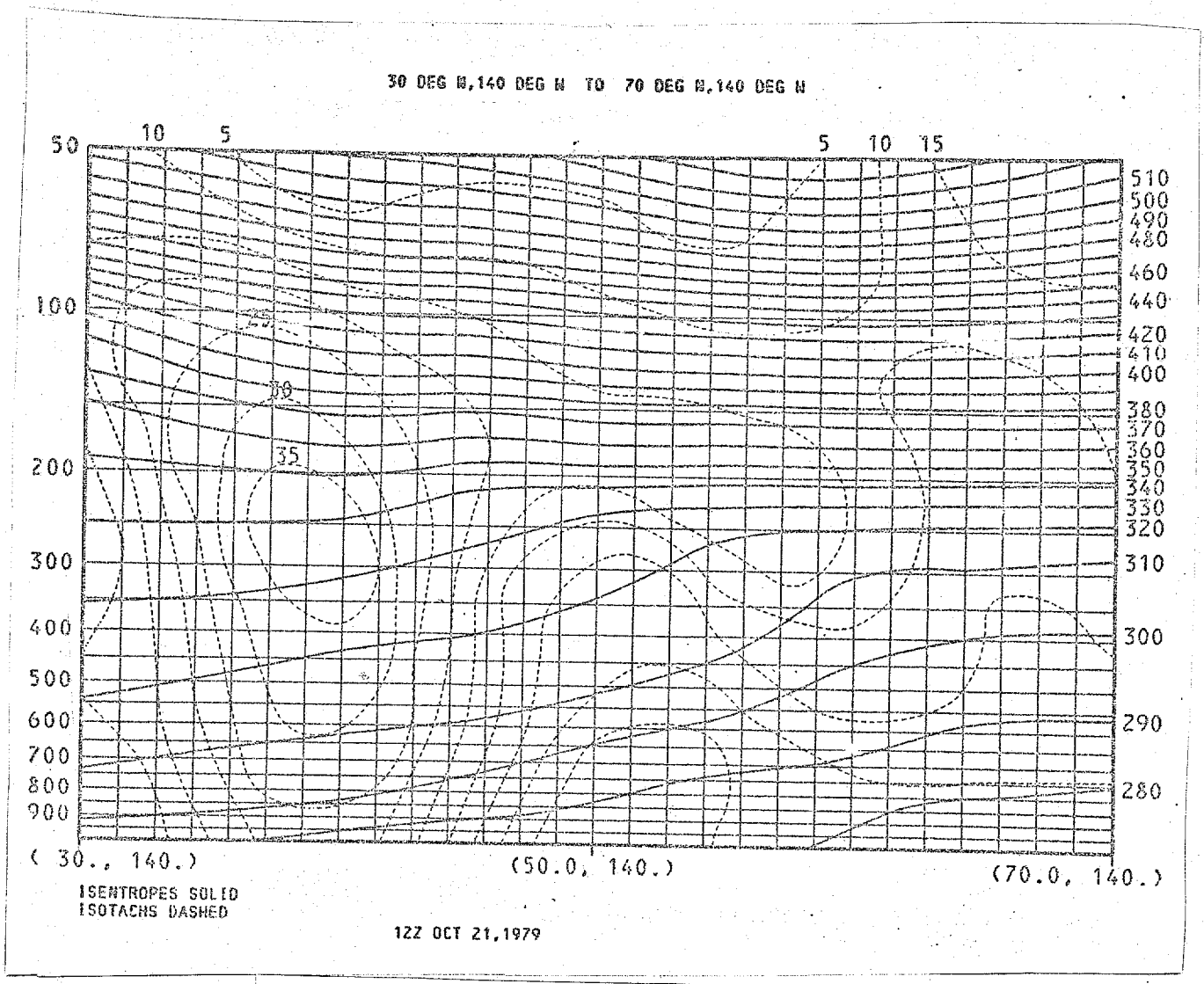

Figure 18. Same as Figure 21, but along 140W.

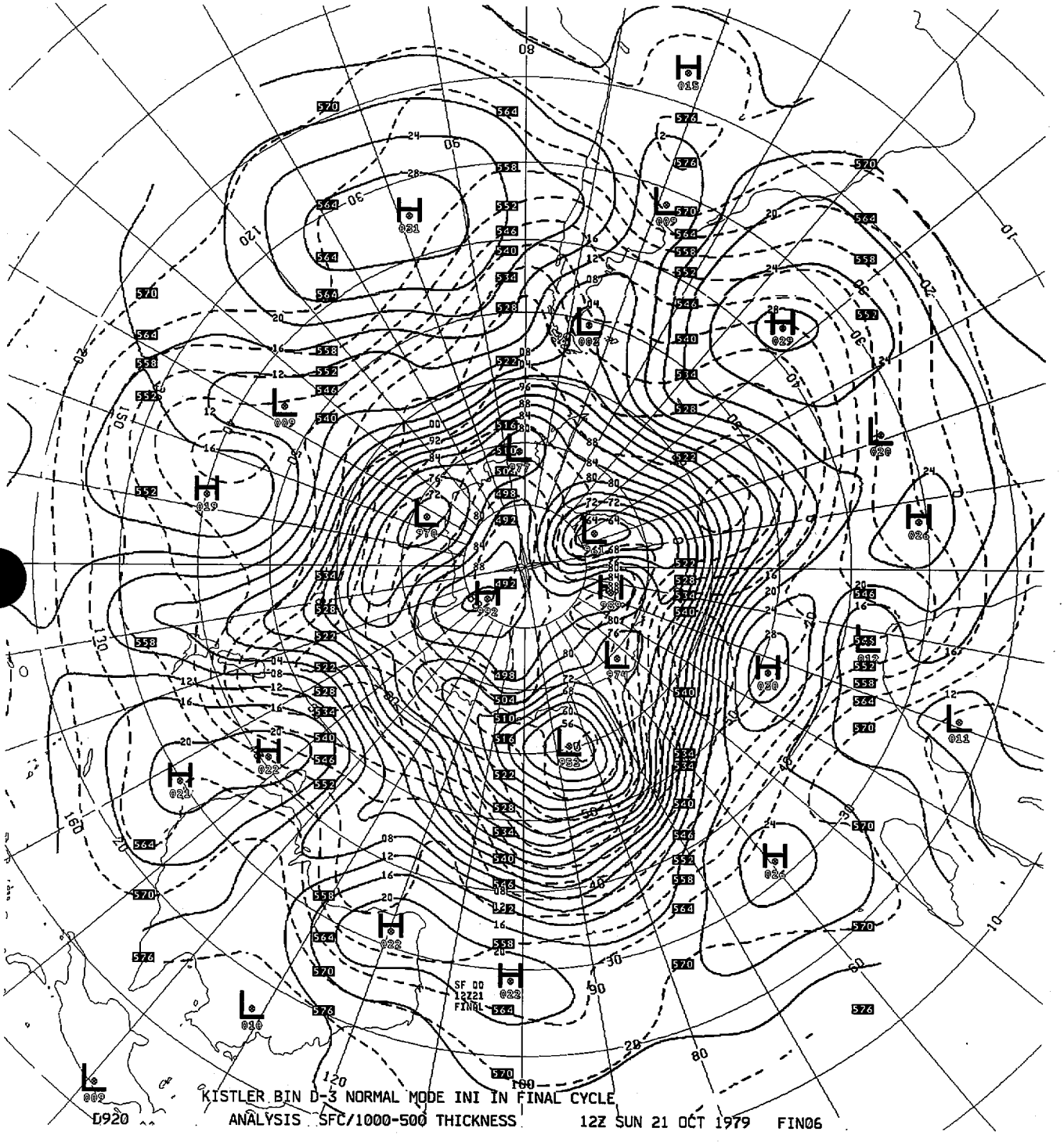

Figure 19. Mean sea level pressure (solid lines, 4 mb interval) and 1000-500 mb thickness (dashed lines, 60 m interval) over the Southern Hemisphere. 1200 GMT 21 October 1979.

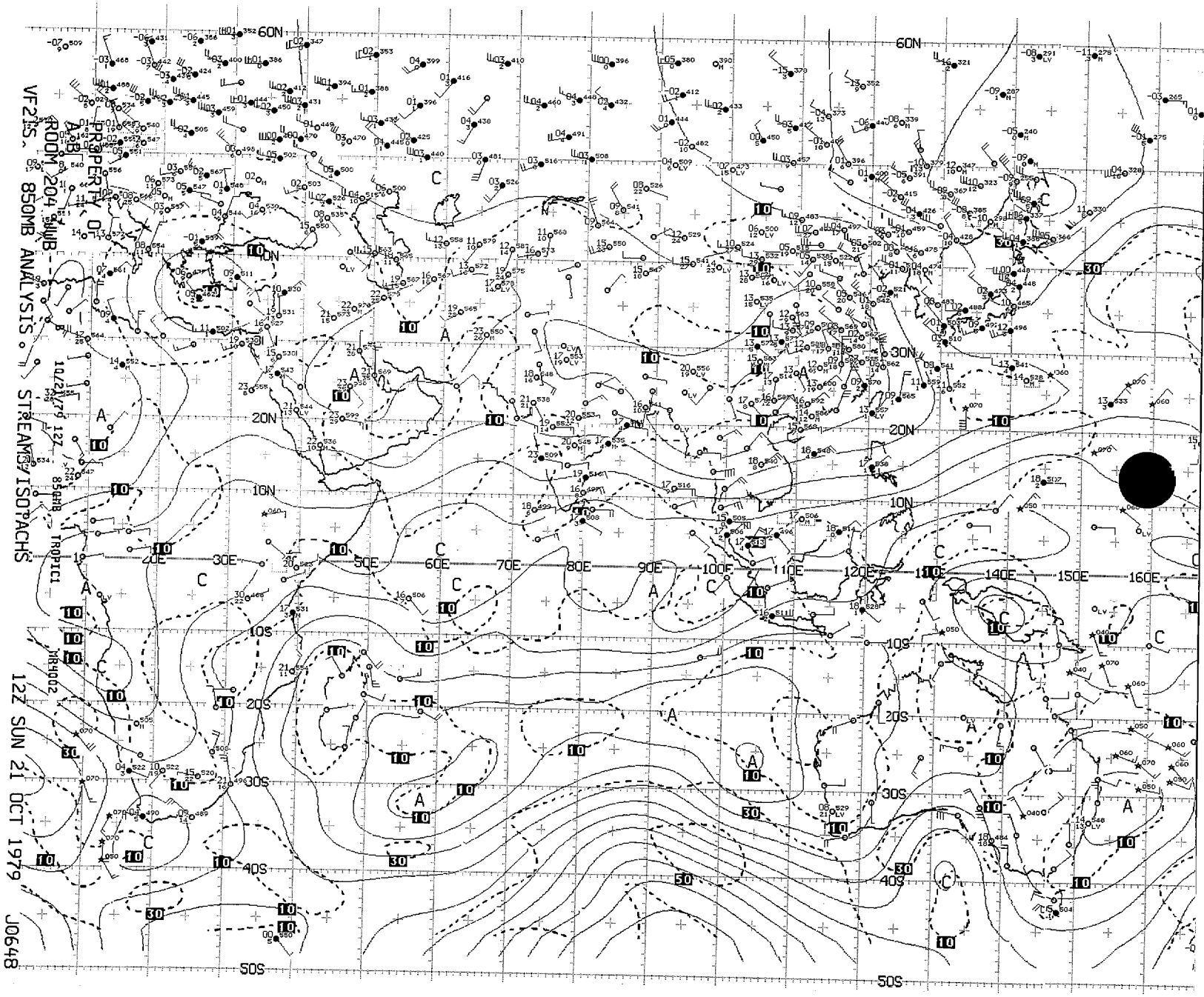

Figure 20. 850-mb streamlines (solid) and isotachs (dashed, 20 kt interval) for 1200 GMT 21 October 1979.

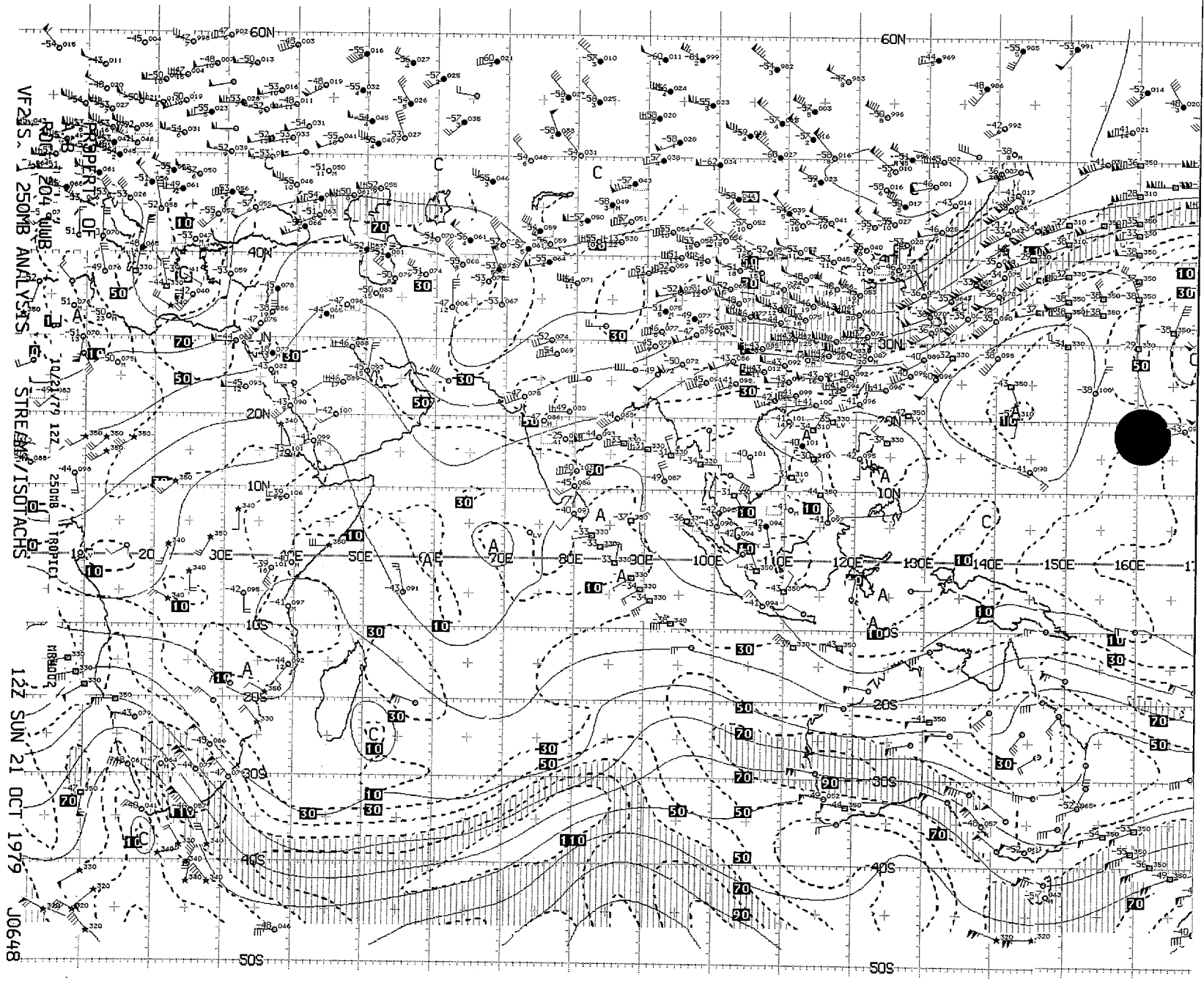

Figure 21. Same as Figure 20, for 250 mb.

V. Summary

This series of lectures began with a review of the evolution of operational objective analysis and data assimilation at the United States Joint Numerical Weather Prediction Unit and the National Meteorological Center. We noted two major forces for change occurring since the mid-1950's: the expansion and changing nature of the data base, and the improvement of prediction models. These factors have made global analysis and prediction possible.

It has also vaulted the prediction model into a dominant role in data assimilation. Because of the general level of skill of modern primitive equation models, it is possible now to consider the prediction model as the main vehicle for carrying a numerical representation of the atmosphere. Corrections to the model's representation are generally of relatively small amplitude and occur on a rather small scale; that is, errors in the long waves in a short period forecast are nearly negligible. One important consequence of this is that the mass field adjusts to the wind field on the scales that appear in the correction field. Accurate wind observations are therefore of primary importance.

Because of the non-homogeneous data base that now exists, recourse has been had to a statistical interpolation procedure to permit systematic blending of data from different sources with the background field. So widespread is the interest in this methodology that two full lectures have been devoted to its theory and application.

Likewise, so important are the changes in the data base that two lectures have been devoted to that subject: first, a series of essays on the main components of the data base; and second, a discussion of the impact of the newer data types on operational numerical prediction.

This final lecture has presented some preliminary evidence on the performance characteristics of the NMC Global Data Assimilation System that has evolved from research in data assimilation over the past decade. We believe it performs reasonably well. We also know it has deficiencies and the "preliminary" evidence noted above refers to the fact that the system will continue to evolve as the deficiencies are eliminated.

References

Gerrity, J., 1979: The Zonally Averaged Final Cycle Circulation on a Day in January. Unpublished NMC manuscript, April 1979.

_____, 1980: A One-Year Statistical Comparison of the Hough and OI Data Assimilation Systems. NMC Office Note 209, January 1980.

Lorenz, E., 1967: The Nature and Theory of the General Circulation of the Atmosphere. World Meteorological Organization, Geneva, 161 pp.

Smith, Stuart M., J. Menand, and G. Sharman, 1965: World Wide Ocean depths and land elevations averaged for one degree squares of latitude and longitude. Scripps Institute of Oceanography Reference Report 65-8.